Smooth Sliding Control Applied to Prosthetic Legs via Variable High Gain Observer

Alessandro J. Peixoto, Ignácio de A. M. Ricart and Matheus Ferreira dos Reis

***Abstract*—This draft focus on state estimation and control of a robot/prosthesis control system with four joints: vertical hip displacement, thigh, knee and ankle angles. The motivation was inspired by several drawbacks regarding the usage of load cells and/or sensors in robots and prosthetic legs to capture gait data, external forces (GRFs) and moments during walking. Thus, state estimation via Extended Kalman Filter (EKF), High-gain-observer (HGO) and Sliding Mode Observer (SMO) are promising as well as the estimation of forces acting on the prosthetic foot. We propose the implementation of an HGO with variable dynamic gain. The key idea is to design a time-varying HGO gain synthesized from measurable signals. This dynamic gain can be designed to: (i) reduce the amount of noise in the control signal while keeping an acceptable tracking error transient performance; (ii) guarantee global/semi-global stability properties of the closed-loop system. The main focus is given to the HGO design while the smooth sliding control scheme is left for a future draft of this note.**

I. Introduction

Prosthesis are devices that substitute the function of a missing limb either due to amputation or a congenital defect. Amputations could occur due to injuries, circulatory and vascular disease, diabetes or cancer and that means a huge number of people that could maintain their activities of daily livings (ADLs) and have the mobility partially / completely restored through improvements in prosthesis technology.

There are three main types of prosthesis currently available: purely passive, active-damping controlled and powered controlled prostheses. The first type requires a significant effort from the amputee because there are only passive mechanical systems to assist him during the gait. Active damping uses microprocessors and sensors to measure when knee flexion and extension is needed based on encoder measures and load transfer acquired from observer/load cells. In this way, it can actively regulate the prosthesis damping factor and help the user during stance phases and during the gait.

A powered controlled prosthesis requires less metabolic energy from the user for walking than purely passive because they are able to generate net power at the joints through DC Motors or pneumatic actuators (ref-Design of a pneumatically actuated transfemoral prosthesis and Actuated leg prosthesis for above knee amputees and Towards a Smart semi-active prosthetic leg preliminary assessment and testing). As they are able to supply positive power, the user could more easily realize tasks such as climbing stairs, walking uphill.

The sensors applied to this type of prosthesis measure the joint angles such as high-resolution rotary encoders and forces such as strain gauges or load cells. Angular velocities could be acquired through expensive tacometers or numerical differentiation. Usually the numerical approach is applied using observers, which have to deal with the challenges of noise rejection.

In the present paper, a proportional-integral-derivative (PID) control method is developed in order to make a robotic prosthetic leg follow a desired walking pattern. A feedback loop, using computed torque, is designed to linearize the plant and an HGO with variable gain is applied to estimate each joint angular velocity.

Output-feedback control strategies using HGOs [1] represent an important design class, in particular those schemes based on time-varying high gain techniques (HGO with variable gain) [2] [3] [4] [5] [6].

In [7], [8], an output-feedback sliding-mode control design have been proposed for arbitrary relative degree uncertain systems, where the class of plants encompasses time-varying minimum phase nonlinear plants, affine in the control, transformable to a normal form and for which a norm state estimator can be implemented. The main objective in [7] was to use a dynamic observer gain in order to obtain global results without invoking the global Lipschitz-like restrictions.

In addition, time-varying HGOs have also been used to cope with the effect of measurement noise and to establish the connections with the Extended Kalman Filter [6] [9].

Considering that the present system has parametric uncertainties and angle measurement is subject to noise, a time-varying HGO design is proposed, similar to [7]. While estimating in real-time the control signal noise, the adaptation law changes the observer gain to achieve a preferable trade-off between control noise and tracking performance. Global results are not pursued in this paper.

This variable gain approach is different from most of the existing techniques, where the HGO gain is updated either solving a Riccati equation [2] [10] [11] or via functions based on measurable signals and norm domination techniques [5], [10], [12] and [7].

The proposed approach is verified in a simulation environment with a 4-link robot/prosthesis system (PRRR), with parameters extracted from [13]. The human gait used as reference signal is obtained from [14].

This paper is organized as follows. In Section III, the system model is described where some considerations regarding the HGO design are taken into. Section IV presents the HGO structure and the adapting function used in simulation. Section V shows the control law applied to the plant and results obtained. Finally, Section VI presents concluding remarks and future work.

II. Preliminaries

The following notations and terminology are used:

- The 2-norm (Euclidean) of a vector x and the corresponding induced norm of a matrix A are denoted by $|x|$ and $|A|$, respectively. The symbol $\lambda[A]$ denotes the spectrum of A and $\lambda_m[A] = -\max_i\{Re\{\lambda[A]\}\}$.
- The $\mathscr{L}_{\infty e}$ norm of a signal $x(t) \in \mathbb{R}^n$ is defined as $\|x_t\| := \sup_{0\leq\tau\leq t}|x(\tau)|$.
- The symbol "s" represents either the Laplace variable or the differential operator "d/dt", according to the context.
- As in [15] the output y of a linear time invariant (LTI) system with transfer function $H(s)$ and input u is given by $y = H(s)u$. Convolution operations $h(t) * u(t)$, with $h(t)$ being the impulse response from $H(s)$, will be eventually written, for simplicity, as $H(s) * u$.
- Classes of $\mathscr{K}, \mathscr{K}_\infty$ functions are defined according to [16, p. 144]. ISS, OSS and IOSS mean Input-State-Stable (or Stability), Output-State-Stable (or Stability) and Input-Output-State-Stable, respectively [17].
- The symbol π denotes class-$\mathscr{KL}$ functions. Eventually, we denote by $\pi(t)$ any exponentially decreasing signal, i.e., a signal satisfying $|\pi(t)| \leq \Pi(t)$, where $\Pi(t) := Re^{-\lambda t}$, $\forall t$, for some scalars $R, \lambda > 0$.

III. System Model

The dynamics of the machine/prosthesis system composed by a 4-link rigid body robot[1] with prismatic-revolute-revolute-revolute (PRRR) configuration, following the notation in [13], is given by:

$$D(q)\ddot{q} + C(q,\dot{q})\dot{q} + B(q,\dot{q}) + P(\dot{q}) + J_e^T F_e + g(q) = F_a\,, \quad (1)$$

where q represents the vector of joints positions (q_1 represents the hip vertical displacement, q_2 is the thigh angle, q_3 is the knee angle and q_4 represents ankle angle), $D(q)$ is the inertia matrix, $C(q,\dot{q})$ is the matrix of Coriolis and centrifugal forces, $B(q,\dot{q})$ is the knee damper nonlinear matrix, J_e is the kinematic Jacobian relative to the point of application of external forces F_e, $g(q)$ is the term of gravitational forces and F_a is the torque/force produced by the actuators. Here, in contrast to [13], we have included the term $P(\dot{q})$ in order to take explicitly into account the Coulomb friction as in [18]. Note that, inertial and frictional effects in the actuators can be included in this model.

To establish a basis for dynamic model derivations and to verify the leg geometry during simulations, the set of reference frames used for forward kinematics problems are the same as the ones assigned in [13]. Matrices $D(q)\ddot{q}$, $C(q,\dot{q})$ and $g(q)$ are obtained using the standard Newton-Euler/Euler-Lagrange approach and are given in Appendix A with the plant parameters extracted from [13].

A. A Simplified Model

In order to illustrate the observer design proposed in this note, consider a simplified version of the machine/prosthesis system (2) where no external forces are considered ($F_e \equiv 0$), the specific leg prosthesis damping matrix is disregarded ($B(q,\dot{q}) \equiv 0$) and the Coulomb friction is neglected ($P(\dot{q}) \equiv 0$). In this case, the machine/prosthesis system is described by:

$$D(q)\ddot{q} + C(q,\dot{q})\dot{q} + g(q) = F_a\,. \quad (2)$$

The system matrices $D(q), C(q,\dot{q})$ and $g(q)$ are supposed to be uncertain, but the corresponding nominal matrices $D_n(q), C_n(q,\dot{q})$ and $g_n(q)$ are assumed known. In particular, the inertia matrix $D(q)$ which is invertible, since $D(q) = D^T(q)$ is strictly positive definite.

Introducing the variables $x_1 := q \in \mathbb{R}^4$ and $x_2 := \dot{q} \in \mathbb{R}^4$, the model (2) can be rewritten in the state-space form as:

$$\begin{aligned} \dot{x}_1 &= x_2\,, & (3)\\ \dot{x}_2 &= k_p(x,t)\,[u + d(x,t)]\,, \quad u := F_a \in \mathbb{R}^{4\times 1}\,, & (4)\\ y &= x_1\,, & (5) \end{aligned}$$

or, equivalently,

$$\begin{aligned} \dot{x} &= A_\rho x + B_\rho k_p(x,t)[u + d(x,t)]\,, & (6)\\ y &= C_\rho x\,, & (7) \end{aligned}$$

where $x^T = \begin{bmatrix} x_1 & x_2 \end{bmatrix}$ is the state vector, $k_p(x,t) = D(x_1)^{-1} \in \mathbb{R}^{4\times 4}$, $d(x,t) := -C(x_1,x_2)x_2 - g(x_1) \in \mathbb{R}^{4\times 1}$, $C_\rho = \begin{bmatrix} I_{4\times 4} & 0_{4\times 4} \end{bmatrix} \in \mathbb{R}^{4\times 8}$ and the pair (A_ρ, B_ρ) is in Brunovskys canonical controllable form and is given by:

$$A_\rho = \begin{bmatrix} 0_{4\times 4} & I_{4\times 4} \\ 0_{4\times 4} & 0_{4\times 4} \end{bmatrix} \in \mathbb{R}^{8\times 8}\,,$$

and

$$B_\rho = \begin{bmatrix} 0_{4\times 4} & I_{4\times 4} \end{bmatrix}^T \in \mathbb{R}^{8\times 4}\,.$$

For each solution of (6) there exists a maximal time interval of definition given by $[0, t_M)$, where t_M may be finite or infinite. Thus, finite-time escape is not precluded, *a priori*.

Remark. (**Nominal Values**) Nominal terms can be used in the HGO implementation in order to reduce conservatism in the HGO design. The plant could be rewritten as:

$$\begin{aligned} \dot{x}_1 &= x_2\,, & (8)\\ \dot{x}_2 &= f(x_1,x_2,u,t) + \delta_f(x_1,x_2,u,t)\,, \quad u := F_a\,, & (9)\\ y &= x_1\,, & (10) \end{aligned}$$

where the nominal part of the system dynamics is represented by

$$f(x_1,x_2,u,t) := D_n^{-1}(x_1)u - D_n^{-1}(x_1)\left[C_n(x_1,x_2)x_2 + g_n(x_1)\right]\,, \quad (11)$$

while the uncertainties are concentrated in the term

$$\delta_f(x_1,x_2,u,t) := \left[D^{-1}(x_1) - D_n^{-1}(x_1)\right]u + \left[D_n^{-1}(x_1)C_n(x_1,x_2) - D^{-1}(x_1)C(x \quad (12)$$

However, to simplify this presentation while keeping the main HGO design methodology, consider $C_n \equiv 0$, $g_n \equiv 0$ and, since D is assumed known, we also have $D_n = D$.

[1] A more general framework with a n-link rigid body robot can also be considered. However, in order to keep this note close to [13], for simplicity, we have set $n = 4$.

IV. High Gain Observer with Variable Gain

The HGO [19] is given by

$$\dot{\hat{x}} = A_\rho \hat{x} + B_\rho k_p^n u + H_\mu L_o (y - C_\rho \hat{x}), \tag{13}$$

where k_p^n is a nominal value of the plant high frequency gain (HFG) k_p and L_o and H_μ are given by:

$$L_o = \begin{bmatrix} l_1 I_{4\times 4} & l_2 I_{4\times 4} \end{bmatrix}^T \in \mathbb{R}^{8\times 4} \tag{14a}$$

$$H_\mu := \mathrm{diag}(\mu^{-1} I_{4\times 4},\ \mu^{-2} I_{4\times 4}) \in \mathbb{R}^{8\times 8}. \tag{14b}$$

The observer gain L_o is such that $s^2 + l_1 s + l_2$ is Hurwitz. In this paper, instead of using a constant μ, we introduce a *variable* parameter $\mu = \mu(t) \neq 0, \forall t \in [0, t_M)$, of the form

$$\mu(\omega, t) := \frac{\bar{\mu}}{1 + \psi_\mu(\omega, t)}, \tag{15}$$

where ψ_μ, named **adapting function**, is a non-negative function continuous in its arguments and ω is an available signal, both to be designed later on. The parameter $\bar{\mu} > 0$ is a design constant. For each system trajectory, μ is absolutely continuous and $\mu \leq \bar{\mu}$. Note that μ is bounded for t in any finite sub-interval of $[0, t_M)$. Therefore,

$$\mu(\omega, t) \in [\underline{\mu}, \bar{\mu}], \quad \forall t \in [t_*, t_M), \tag{16}$$

for some $t_* \in [0, t_M)$ and $\underline{\mu} \in (0, \bar{\mu})$.

A. High Gain Observer Error Dynamics

The transformation [1]

$$\zeta := T_\mu \tilde{x}, \quad T_\mu := [\mu^2 H_\mu]^{-1} \in \mathbb{R}^{8\times 8}, \quad \tilde{x} := x - \hat{x}, \tag{17}$$

is fundamental to represent the $\tilde{x}$-dynamics in convenient coordinates allowing us to show that $\tilde{x}$ is arbitrarily small, *modulo* exponentially decaying term. First, note that:

$$(i)\ T_\mu (A_\rho - H_\mu L_o C_\rho) T_\mu^{-1} = \frac{1}{\mu} A_o, \quad (ii)\ T_\mu B_\rho = B_\rho,$$

$$\text{and} \quad (iii)\ \dot{T}_\mu T_\mu^{-1} = \frac{\dot{\mu}}{\mu} \Delta,$$

where $A_o := A_\rho - L_o C_\rho$ and $\Delta := \mathrm{diag}(-I_{4\times 4},\ 0_{4\times 4}) \in \mathbb{R}^{8\times 8}$. Then, subtracting (13) from (6) and applying the above relationships (i), (ii) and (iii), the dynamics of $\tilde{x}$ in the new coordinates ζ (17) is given by:

$$\mu \dot{\zeta} = [A_o + \dot{\mu}(t)\Delta]\zeta + B_\rho [\mu \nu], \tag{18}$$

where

$$\nu := (k_p - k_p^n) u + k_p d, \tag{19}$$

and

$$\dot{\mu}(t) = -\frac{\mu^2}{\bar{\mu}} \left[\frac{\partial \psi_\mu}{\partial \omega} \dot{\omega} + \frac{\partial \psi_\mu}{\partial t} \right]. \tag{20}$$

The HGO gain ($H_\mu L_o$) is inversely proportional to the small parameter μ, allowed to be time-varying. Our task is to establish properties for the adapting function $\psi_\mu(\omega, t)$ in (15) so that $\mu|\nu|$ and $|\dot{\mu}|$ are arbitrarily small, at least after a finite time interval. In fact, we design ψ_μ so that the following inequalities hold

$$|\dot{\mu}(t)|,\ \mu|\nu| \leq \mathscr{O}(\bar{\mu}), \quad \forall t \in [t_\mu, t_M). \tag{21}$$

for some finite $t_\mu \in [0, t_M)$. Consequently, $\dot{\mu}$ does not *ultimately* affect the stability of A_o in (18) and ζ can be made arbitrarily small, *modulo* an exponentially decaying term, by applying a time scale changing in (18). In addition, since $\tilde{x} = T_\mu^{-1} \zeta$ and $\|T_\mu^{-1}\|$ is of order $\mathscr{O}(1)$, then one can conclude that $\tilde{x}$ can also be made arbitrarily small, *modulo* an exponentially decaying term.

It is clear that inequalities in (21) depend on the choice of the control signal u in (19), the disturbance and the signal ω.

B. The Adapting Function ψ_μ

The adapting function $\psi_\mu(\omega, t)$ used in the time-varying parameter

$$\mu(\omega, t) := \frac{\bar{\mu}}{1 + \psi_\mu(\omega, t)}, \tag{22}$$

defined in (15), can assume different forms depending on the choice of the signal ω and the available information about the plant.

As an example, consider the following cases:

1) **From a theoretical point of view**: the adapting function ψ_μ can be chosen in order to allow global/semi-global stability (or only convergence) properties for the closed-loop control system.
   a) **Norm Observability**: The plant (6)–(7) admits a norm observer which provides an upper bound for the plant state norm by using only available signals: plant input (u) and plant output (y). In this case, global or semi-global results could be obtained when, for example, a sliding mode based control is employed, as in [7].
   More precisely, a norm observer for system (6)–(7) is a m-order dynamic system of the form:

$$\tau_1 \dot{\omega}_1 = -\omega_1 + u, \tag{23}$$

$$\tau_2 \dot{\omega}_2 = \gamma_o(\omega_2) + \tau_2 \varphi_o(\omega_1, y, t), \tag{24}$$

   with states $\omega_1 \in \mathbb{R}$, $\omega_2 \in \mathbb{R}^{m-1}$ and positive constants τ_1, τ_2 such that for $t \in [0, t_M)$: (i) if $|\varphi_o|$ is uniformly bounded by a constant $c_o > 0$, then $|\omega_2|$ can escape at most exponentially and there exists $\tau_2^*(c_o)$ such that the ω_2-dynamics is BIBS (Bounded-Input-Bounded-State) stable w.r.t. φ_o for $\tau_2 \leq \tau_2^*$; (ii) for each $x(0), \omega_1(0), \omega_2(0)$, there exists $\bar{\varphi}_o$ such that

$$|x(t)| \leq \bar{\varphi}_o(\omega(t), t) + \pi_o(t), \quad \omega := [\omega_1\ \omega_2^T\ y]^T, \tag{25}$$

   where $\pi_o := \beta_o(|\omega_1(0)| + |\omega_2(0)| + |x(0)|) e^{-\lambda_o t}$ with some $\beta_o \in \mathscr{K}_\infty$ and positive constant λ_o.
   b) **The system states can be assumed bounded**: The plant state, in particular the unavailable state x_2, is uniformly bounded. Such assumption of the state boundedness is true, for example, when (6) is BIBS stable, and the control input is bounded. Moreover, by considering that the acceleration ($\dot{x}_2$) in the mechanical system is bounded by a known constant, then a constant

upper bound for the velocity x_2 can be found by using the "dirty derivative":

$$\eta := \frac{s}{\tau s+1} y. \tag{26}$$

Indeed, by noting that

$$x_2 = \eta + \frac{\tau}{\tau s+1}\dot{x}_2\,, \tag{27}$$

one can obtain the following norm bound

$$|x_2| \leq |\eta| + \mathscr{O}(\tau)\,|\dot{x}_2|\,. \tag{28}$$

In this case, we can use this rough estimate for x_2 and less conservative estimates for the terms depending on y, so that ω can be implemented.

2) **From a practical point of view**: one can select a time-varying adapting function ψ_μ to assure an acceptable level of noise in the control signal while keeping a good transient for the output tracking error.
   a) **Signal-to-Noise Ratio in $|u|$ $\times$ Tracking Error Norm**: By using some measurement of the amount of noise in the control signal, for example, the Signal-to-Noise Ratio (SNR), the adapting function can be implemented as a function of the SNR and the tracking error, so that μ increases when the SNR in the control effort increases and μ decreases when the tracking error norm increases. This can be accomplished, for example, by defining a cost function depending on the control signal-to-noise ratio and the output tracking error, so that the time-varying μ reaches an optimum value.

C. One Particular Design for ψ_μ via Domination Techniques

When the plant (6)–(7) admits a norm observer with ω defined in (25) such that

$$|x(t)| \leq \bar{\varphi}_o(\omega(t),t) + \pi_o(t)\,, \tag{29}$$

and a sliding mode based control is employed, then the signal ν satisfies (see [7] for details):

$$|\nu| \leq \psi_\nu(\omega,t) + \pi_3\,, \tag{30}$$

for some non-negative function ψ_ω and vanishing term π_3 depending on initial conditions. Moreover, the signal ω is such that the following inequality holds (see [7] for details):

$$|\dot{\omega}| \leq \psi_\omega(\omega,t) + \pi_1\,, \tag{31}$$

respectively, for some non-negative functions ψ_ω and vanishing terms π_1 depending on initial conditions. In order to obtain a norm bound for the time derivative of μ (15) we calculate $\dot{\mu}$ by the expression:

$$\dot{\mu}(t) = -\frac{\mu^2}{\bar{\mu}}\left[\frac{\partial \psi_\mu}{\partial \omega}\dot{\omega} + \frac{\partial \psi_\mu}{\partial t}\right]. \tag{32}$$

Note that, $\dot{\mu}$ is a piecewise continuous time signal which can be upperbounded by

$$|\dot{\mu}(t)| \leq \frac{\left|\frac{\partial \psi_\mu}{\partial \omega}\right|}{1+\psi_\mu}\mu|\dot{\omega}| + \frac{\left|\frac{\partial \psi_\mu}{\partial t}\right|}{1+\psi_\mu}\mu\,. \tag{33}$$

Hence, one has that:

$$\mu|\nu| \leq \frac{\psi_\nu}{1+\psi_\mu}\bar{\mu} + \mu\pi_3\,, \tag{34}$$

and

$$\mu|\dot{\omega}| \leq \frac{\psi_\omega}{1+\psi_\mu}\bar{\mu} + \mu\pi_1\,. \tag{35}$$

Now, choose the adapting function ψ_μ in (15) so that the following property holds with ψ_ν in (30) and ψ_ω in (31):

(P0) $\psi_\nu\,,\ \psi_\omega \leq c_{\mu 0}(1+\psi_\mu)$, $\forall t \in [0,t_M)$, where $c_{\mu 0} \geq 0$ is a *known* constant.

If ψ_μ satisfies (P0) then, from (34) and (35), $\mu|\nu|$ and $\mu|\dot{\omega}|$ can be bounded by

$$\mu|\nu| \leq \mathscr{O}(\bar{\mu}) + \mu\pi_3\,. \tag{36}$$

$$\mu|\dot{\omega}| \leq \mathscr{O}(\bar{\mu}) + \mu\pi_1\,. \tag{37}$$

Moreover, our strategy is to design $\psi_\mu(\omega,t)$ such that the following property holds:

(P1) $\left|\frac{\partial \psi_\mu}{\partial \omega}\right|\,,\ \left|\frac{\partial \psi_\mu}{\partial t}\right| \leq c_{\mu 1}(1+\psi_\mu)$, $\forall t \in [0,t_M)$, where $c_{\mu 1} \geq 0$ is a *known* constant.

This property is trivially satisfied by polynomial ψ_μ with positive coefficients. Now, with ψ_μ satisfying (P1), one has that:

$$|\dot{\mu}(t)| \leq c_{\mu 1}\mu|\dot{\omega}| + c_{\mu 1}\mu\,. \tag{38}$$

Therefore, from (38), (36) and (37) the following holds:

$$|\dot{\mu}(t)|\,,\ \mu|\nu| \leq \mathscr{O}(\bar{\mu}) + \mu\pi_4\,, \tag{39}$$

where $\pi_4 := c_{\mu 1}\pi_1 + \pi_3$.

Finally, if ψ_μ is designed so that (P0)–(P1) hold and *finite escape is avoided*[2], then from (39) one can verify that there exists a finite $t_\mu \in [0,t_M)$ such that:

$$|\dot{\mu}(t)|\,,\ \mu|\nu| \leq \mathscr{O}(\bar{\mu})\,, \quad \forall t \in [t_\mu, t_M)\,. \tag{40}$$

In this case, the stability and/or convergence analysis can be carried out by noting that the output tracking error dynamics (and the full error system dynamics) is ISS w.r.t. HGO estimate error $\tilde{x}$ which is of order $\mathscr{O}(\bar{\mu})$ after the small finite time instant t_μ.

V. Numerical Simulations

The control objective is to reduce the tracking error

$$e(t) := y_d - y\,, \tag{41}$$

where the desired trajectory y_d is ideally a set of joint angles acquired for human gait analysis [14]. For simplicity a second-order filter with transfer function

$$H(s) = \frac{w_n^2}{s^2 + 2\zeta\omega_n + \omega_n^2} \tag{42}$$

[2]This can be guaranteed if an additional technical Property is satisfied, see [7] for details. Here, we omitted this property just to simplify the paper presentation.

has been designed so that the reference signal is actually a filtered version of human gait angles. Through this approach, time-varying derivatives ($\dot{y}_d$ and $\ddot{y}_d$) from the filtered signal are easily acquired and with no error or delay. The plant initial conditions are: $y(0) = x_1(0) = \begin{bmatrix} 0.0216 & 0.5675 & -0.13 & -0.39 \end{bmatrix}^T$ and $x_2(0) = \begin{bmatrix} 0 & 0 & 0 & 0 \end{bmatrix}^T$.

A PID controller with feedforward is employed just to validate the time-varying HGO proposed in this note. By recalling that we consider $D_n(y) = D(y)$ to simplify the paper presentation, the control signal is given by

$$u(t) := D(y)u_v + C_n(y,\hat{x}_2)\hat{x}_2 + g_n(y)\,, \tag{43}$$

$$u_v(t) := \ddot{q}_d + K_p e(t) + \underbrace{K_d(\dot{y}_d - \hat{x}_2)}_{\approx K_d \frac{de(t)}{dt}} + K_i \int_{t_o}^{t} e\,dt\,, \tag{44}$$

where $\hat{x}_2$ is the estimate for x_2 obtained from the HGO and the gains were designed in order to match the following equations

$$s^3 + K_d s^2 + K_p s + K_i = 0 \tag{45}$$

$$(s^2 + 2\zeta\omega_n + \omega_n^2)(s+p) = 0 \tag{46}$$

$$\tag{47}$$

Therefore the controller gains are designed in order to approximate the erro third order dynamics to a second order system added to a fast pole. That will accomplished if

$$k_i := \omega_n^2 p \tag{48}$$

$$k_p := \omega_n^2 + 2\zeta\omega_n p \tag{49}$$

$$k_d := p + 2\zeta\omega_n \tag{50}$$

where $\omega_n = 16\pi$, $\zeta = 0.9$, $p = 2\omega_n$, $K_i := k_i(I_{4\times4})$, $K_p := k_p(I_{4\times4})$ and $K_d := k_d(I_{4\times4})$.

Note that, in the ideal case when the nominal matrices C_n and g_n match the real values and $\hat{x}_2 = x_2$, the following closed-loop equation holds

$$\dddot{e} + K_d\ddot{e} + K_p\dot{e} + K_i e = 0\,, \tag{51}$$

which, with gains chosen such that $s^3 + K_d s^2 + K_p s + K_i = 0$ is Hurwitz, assures that $|e(t)| \to 0$ as $t \to \infty$. When there are uncertainties in the plant parameters and/or errors in the HGO estimate, the tracking error converges to some residual set.

In the present case, it is considered a random parametric error in plant parameters from [13] such as center of gravity, inertia matrix, link length. But the values won't differ by more than 10% from the real value.

The HGO is implemented with $l_1 = 2$, $l_2 = 6$ and with a constant $\mu = \bar{\mu} = 0.001$.

In Fig. 1, Fig. 2, Fig. 3 and Fig. 4 it can be noticed that each joint has its own trajectory and initial condition, which affect differently the estimated state overshoot before convergence. However, every position estimative converges at approximately 7 ms and the highest overshoot happens in the thigh angle because of its initial condition error (0.57π).

Due to parametrical errors and high frequency dynamics, the highest tracking error happens on the ankle angle, which takes more than 100ms to converge. Anothe interesting tracking error behaviour occurs at hip displacement while changing orientation with all the system inertia, causing a higher tracking error than in any other moment and also making the control signal to even saturate in order to follow the trajectory.

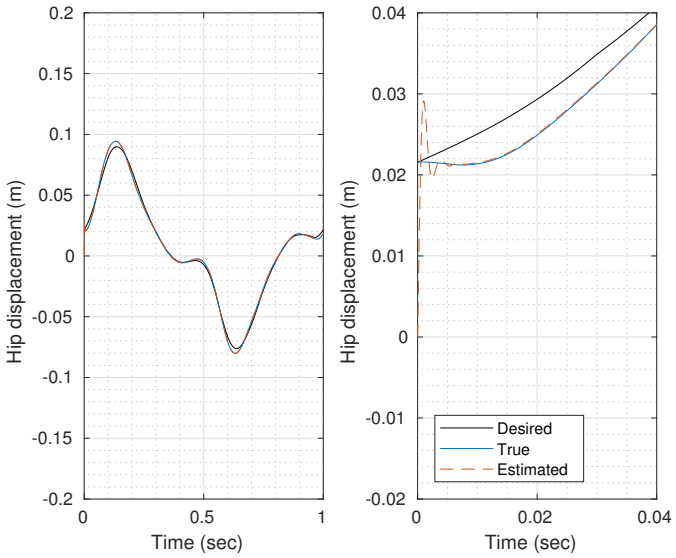

Fig. 1. Simulation results from a desired hip movement, the controlled plant state and the estimated state from the HGO with constant parameter $\mu = 0.001$. The right plot shows the signals behaviours until the first 40ms of simulation

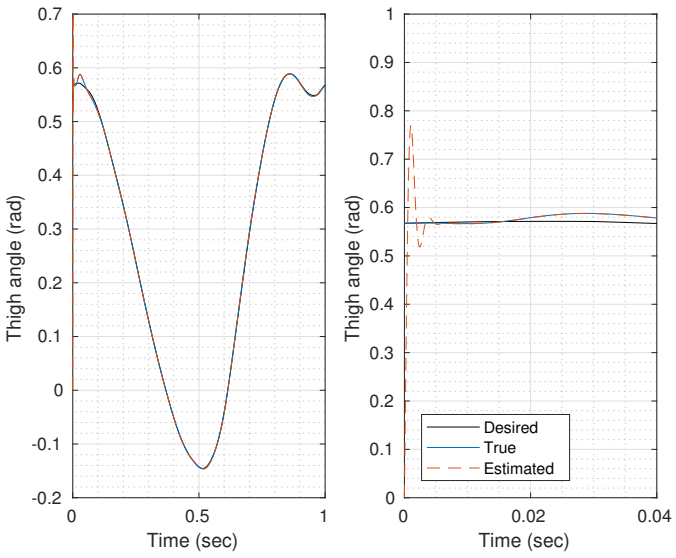

Fig. 2. Simulation results from a desired thigh movement, the controlled plant state and the estimated state from the HGO with constant parameter $\mu = 0.001$. The right plot shows the signals behaviours until the first 40ms of simulation

The corresponding hip, thigh, knee and ankle velocities are illustrated in Fig. 5, Fig. 6, Fig. 7 and Fig. 8, respectively. The RMSE for tracking error in Table. I shows that velocities in knee and ankle joints require a faster control law to track. That happens because of higher frequency components which also contribute to a worst state estimation in HGO. Now, in order to illustrate one possible scenario in which the time-varying HGO parameter can be used, the plant parameters are

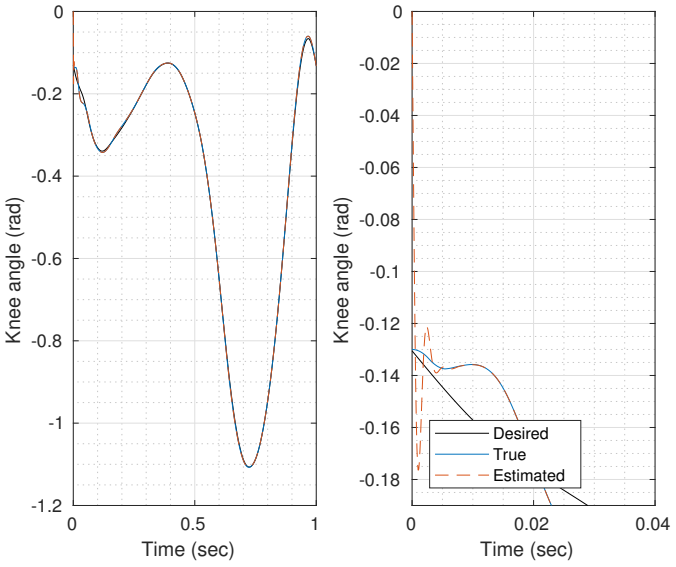

Fig. 3. Simulation results from a desired knee movement, the controlled plant state and the estimated state from the HGO with constant parameter $\mu = 0.001$. The right plot shows the signals behaviours until the first 40ms of simulation

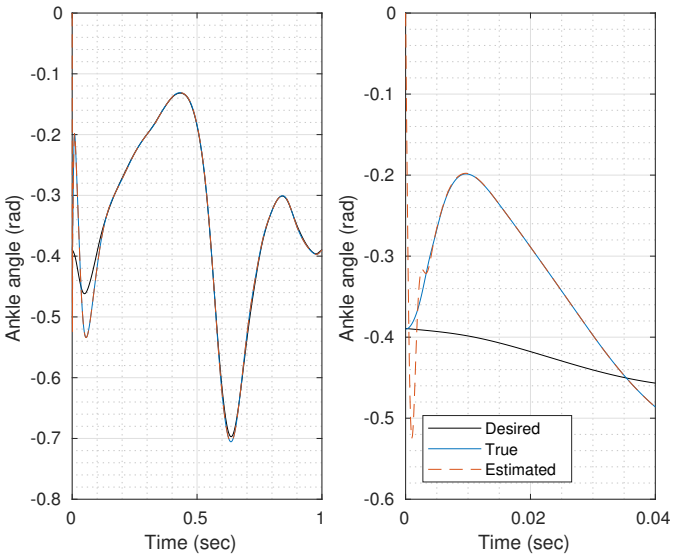

Fig. 4. Simulation results from a desired ankle movement, the controlled plant state and the estimated state from the HGO with constant parameter $\mu = 0.001$. The right plot shows the signals behaviours until the first 40ms of simulation

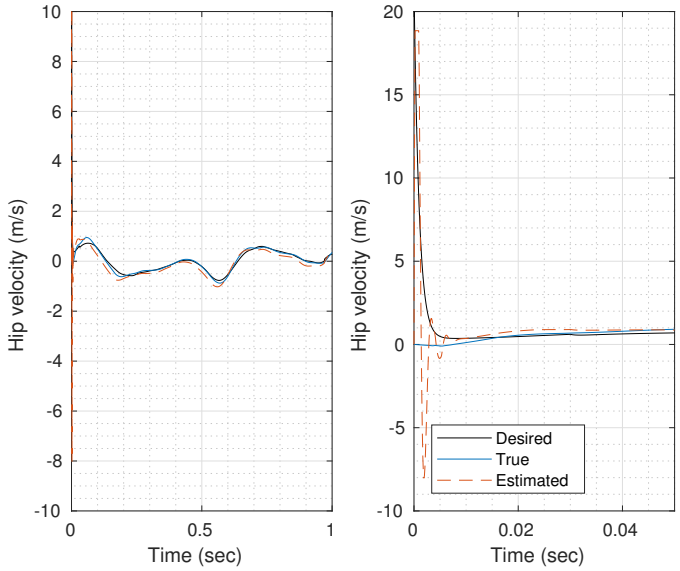

Fig. 5. Simulation results from a desired hip velocity, the controlled plant state and the estimated state from the HGO with constant parameter $\mu = 0.001$. The right plot shows the signals behaviours until the first 15ms of simulation.

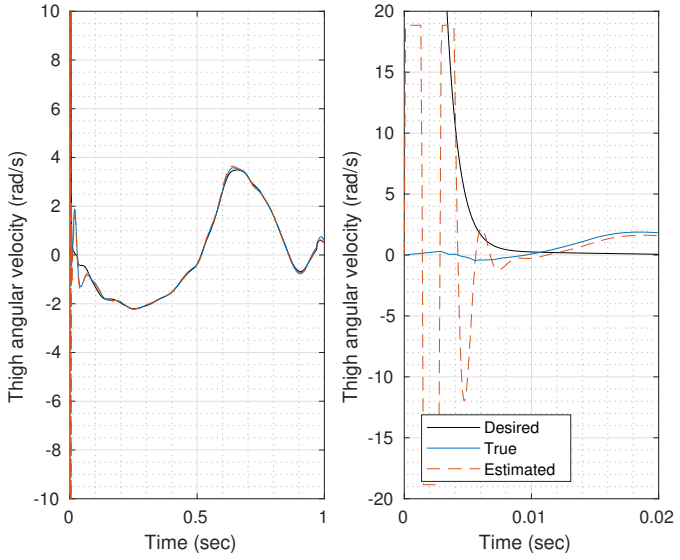

Fig. 6. Simulation results from a desired thigh velocity, the controlled plant state and the estimated state from the HGO with constant parameter $\mu = 0.001$. The right plot shows the signals behaviours until the first 15ms of simulation.

known with parametric error. In order to observe the effect of the input disturbance, a large but unknown constant input disturbance is employed during the whole simulation.

There is an integral action implemented in the control scheme, therefore the input disturbance causes a transient in the tracking error and any steady state error will be compensated. This transient increases as μ increases and it is useful to illustrate the usage of the time-varying parameter μ.

By applying a constant value of $\mu(t) = 1.9e-3$ an apparent degradation in the closed-loop tracking error transient is observed in Fig. **??** (a). On the other hand, the noise amplitude in the control signal is acceptable as can be observed in Fig. **??** (b) with the corresponding measurement of the noise amplitude illustrated in Fig. **??** (c). The noise amplitude was obtained by filtering the control input u with a high-pass filter.

By reducing μ to the constant small value $\mu(t) = 4e-4$, the tracking error transient is improved in exchange of an increase on the control signal noise, see Fig. **??** (a), (b) and (c).

On the other hand, when the time-varying $\mu(t)$ is implemented starting with the same large value for $\bar{\mu} = 0.1$, the tracking error transient is improved, see Fig. **??** (a), without reducing μ to a prohibitive value which can cause a large noise in the control signal, as illustrated in Fig. **??** (b) and (c).

In this case, the time evolution of $\mu(t)$ is shown in

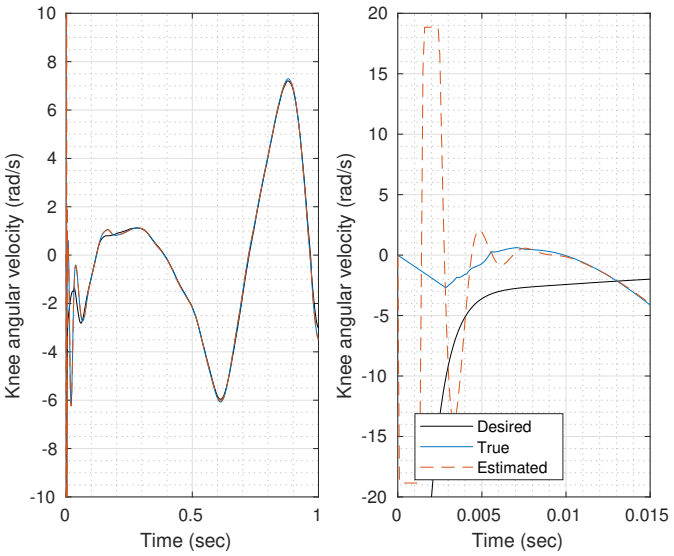

Fig. 7. Simulation results from a desired knee velocity, the controlled plant state and the estimated state from the HGO with constant parameter $\mu = 0.001$. The right plot shows the signals behaviours until the first 15ms of simulation.

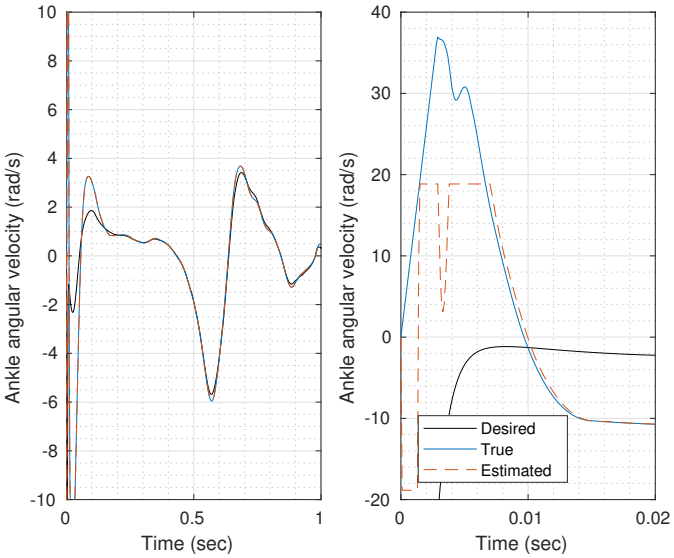

Fig. 8. Simulation results from a desired ankle velocity, the controlled plant state and the estimated state from the HGO with constant parameter $\mu = 0.001$. The right plot shows the signals behaviours until the first 15ms of simulation.

Fig. 10 (a), from which one can verify that μ reaches a value of $\mu_{var} = 1e-3$ depending on the noise power applied to the system. This value is not known *a priori*. It is clear that care must be taken while reducing $\bar{\mu}$, since there exists a trade off between noise reduction and tracking accuracy.

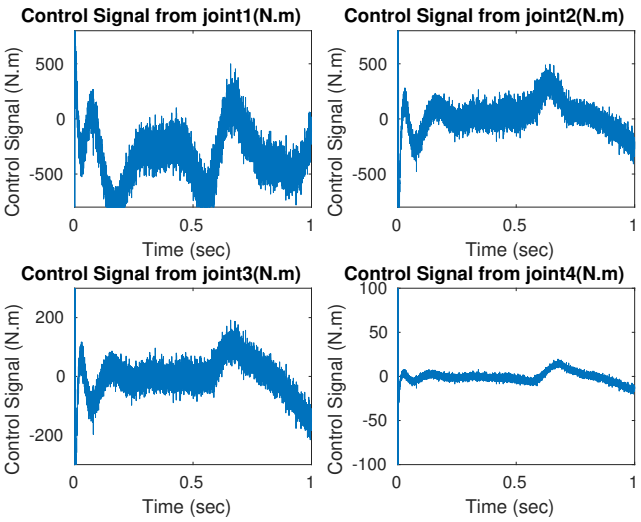

Fig. 9. Simulation results. $\mu = 4e-04$.

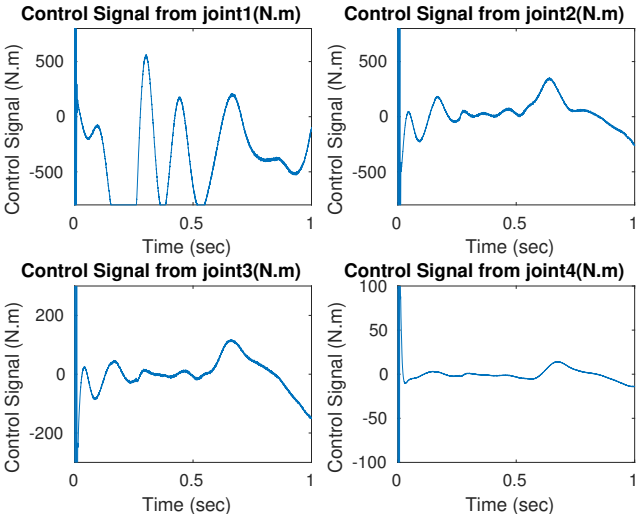

Fig. 10. Simulation results. $\mu = 19e-04$.

VI. Conclusions and Future Work

In this note, we considered the state estimation problem of a robot/prosthesis control system with vertical hip displacement, thigh angle and knee angle. It was verified that it is possible to apply HGO with dynamic gain in order to reduce the amount of noise in the control signal while assuring an reasonable output tracking error transient. Moreover, when a norm observer is available, domination techniques can be used to design the HGO dynamic gain to obtain global/semi-global practical tracking. An illustrative academic simulation example was presented.

TABLE I

Tracking root-mean-square-error (RMSE) of a human gait for each joint of a prosthetic leg with estimated states according to the observer gain μ

μ	x_1 (m)	x_2 (rad)	x_3 (rad)	x_4 (rad)	$\dot{x}_1$ (m/s)	$\dot{x}_2$ (rad/s)	$\dot{x}_3$ (rad/s)	$\dot{x}_4$ (rad/s)
0.4e-3	0.0004	0.0002	0.0009	0.0004	0.0159	0.0117	0.0959	0.0492
1.9e-3	0.0035	0.0013	0.0033	0.0062	0.1120	0.0587	0.2405	0.6836
Variable	0.0008	0.0004	0.0025	0.0059	0.0257	0.0375	0.2268	0.6640

TABLE II

Estimation root-mean-square-error (RMSE) of a human gait for each joint of a prosthetic leg with estimated states according to the observer gain μ

μ	x_1 (m)	x_2 (rad)	x_3 (rad)	x_4 (rad)	$\dot{x}_1$ (m/s)	$\dot{x}_2$ (rad/s)	$\dot{x}_3$ (rad/s)	$\dot{x}_4$ (rad/s)
0.4e-3	0.0001	0.0036	0.0008	0.0024	0.2607	0.4228	0.3570	0.4065
1.9e-3	0.0004	0.0065	0.0015	0.0045	0.3973	0.7754	0.5952	0.8514
Variable	0.0003	0.0065	0.0015	0.0045	0.3167	0.7724	0.5948	0.8512

Future possible topics of research are: (i) consider the full robot/prosthesis model including the ground reaction forces and the ankle joint and its estimation; (ii) verify if it is possible to obtain a norm bound for the system state in order to assure global/semi-global stability properties; (iii) design and implementation of the smooth sliding control scheme and (iv) perform experimental results.

REFERENCES

[1] S. Oh and H. K. Khalil, "Nonlinear output-feedback tracking using high-gain observer and variable structure control," *Automatica*, vol. 33, no. 10, pp. 1845–1856, 1997.

[2] L. Praly, "Asymptotic stabilization via output feedback for lower triangular systems with output dependent incremental rate," in *Proc. IEEE Conf. on Decision and Control*, Orlando, Florida USA, 2001, pp. 3808–3813.

[3] P. Krishnamurthy, F. Khorrami, and Z. P. Jiang, "Global output feedback tracking for nonlinear systems in generalized output-feedback canonical form," *IEEE Trans. Aut. Contr.*, vol. 47, no. 5, pp. 814–819, 2002.

[4] P. Krishnamurthy, F. Khorrami, and R. S. Chandra, "Global high-gain-based observer and backstepping controller for generalized output-feedback canonical form," *IEEE Trans. Aut. Contr.*, vol. 48, no. 12, pp. 2277–2284, 2003.

[5] H. Lei and W. Lin, "Universal output feedback control of nonlinear systems with unknown growth rate," in *Preprints of the 16th IFAC World Congress*, Prague, Czech Republic, July 2005.

[6] J. H. Ahrens and H. K. Khalil, "Closed-loop behavior of a class of nonlinear systems under EKF-based control," *IEEE Trans. Aut. Contr.*, vol. 52, no. 3, pp. 536–540, 2007.

[7] A. J. Peixoto, T. R. Oliveira, and L. Hsu, "Global tracking sliding mode control for a class of nonlinear systems via variable gain observer," *International Journal of Robust and Nonlinear Control*, pp. 177–196, 2011.

[8] A. J. Peixoto, L. Hsu, R. R. Costa, and F. Lizarralde, "Global tracking sliding mode control for uncertain nonlinear systems based on variable high gain observer," in *Proc. IEEE Conf. on Decision and Control*, New Orleans, LA, USA, 2007, pp. 2041–2046.

[9] J. H. Ahrens and H. K. Khalil, "High-gain observers in the presence of measurement noise: A switched-gain approach," *Automatica*, vol. doi:10.1016/j.automatica.2008.11.012, 2009.

[10] V. Andrieu, L. Praly, and A. Astolfi, "Asymptotic tracking of a state trajectory by output-feedback for a class of non linear systems," in *CDC*, New Orleans, LA, USA, 2007, pp. 5228–5233.

[11] G. Kaliora, A. Astolfi, and L. Praly, "Norm estimators and global output feedback stabilization of nonlinear systems with ISS inverse dynamics," *IEEE Trans. Aut. Contr.*, vol. 51, no. 3, pp. 493–498, 2006.

[12] V. Andrieu, L. Praly, and A. Astolfi, "High gain observers with updated gain and homogeneous correction terms," *Automatica*, vol. 45, no. 2, pp. 422–428, 2009.

[13] H. Richter, D. Simon, W. A. Smith, and S. Samorezov, "Dynamic modeling, parameter estimation and control of a leg prosthesis test robot," *Applied Mathematical Modelling*, vol. 39, no. 2, pp. 559–573, 2015.

[14] M. H. Schwartz, A. Rozumalski, and J. P. Trost, "The effect of walking speed on the gait of typically developing children," *Journal of Biomechanics*, vol. 41, no. 8, pp. 1639 – 1650, 2008. [Online]. Available: http://www.sciencedirect.com/science/article/pii/S0021929008001450

[15] P. Ioannou and J. Sun, *Robust Adaptive Control*. Prentice-Hall, 1996.

[16] H. K. Khalil, *Nonlinear Systems*, 3rd ed. Prentice Hall, 2002.

[17] E. D. Sontag and Y. Wang, "On characterizations of the input-to-state stability property," *Systems & Contr. Letters*, vol. 24, pp. 351–359, 1995.

[18] J. Lee, R. Mukherjee, and H. K. Khalil, "Output feedback stabilization of inverted pendulum on a cart in the presence of uncertainties," *Automatica*, vol. 54, pp. 146–157, 2015.

[19] H. K. Khalil, "High-gain observers in nonlinear feedback control," *2008 International Conference on Control, Automation and Systems*, pp. xlvii – lvii, 2008.

APPENDIX

A. System Matrices and Parameters

The plant parameters are given in Table III, while the matrices $D(q), C(q,\dot{q})$ and $g(q)$, appearing in (1), are given by:

$$
\begin{aligned}
C(1,1) &= C(2,1) = C(3,1) = C(3,3) = 0\,,\\
C(1,2) &= -\dot{q}_2(L_2m_3 + m_2(C_2+L_2))\sin(q_2) - C_3m_3(\dot{q}_2+\dot{q}_3)\sin(q_2+q\\
C(1,3) &= -C_3m_3\sin(q_2+q_3)(\dot{q}_2+\dot{q}_3)\,,\\
C(2,2) &= -C_3L_2m_3\dot{q}_3\sin(q3)\,,\\
C(2,3) &= -C_3L_2m_3\sin(q_3)(\dot{q}_2+\dot{q}_3)\,,\\
C(3,2) &= C_3L_2m_3\dot{q}_2\sin(q_3)\,,
\end{aligned}
\qquad (
$$

$$
\begin{aligned}
D(1,1) &= m_1+m_2+m_3\,,\\
D(1,2) &= D(2,1) = (c_3\cos(q_2+q_3)+l_2\cos(q_2)) + m_2(c_2\cos(q_2)+l_2\,c\\
D(1,3) &= D(3,1) = c_3m_3\cos(q_2+q_3)\,,\\
D(2,2) &= I_{2z}+I_{3z}+c_2^2m_2+c_3^2m_3+I_2^2(m_2+m_3)+2c_2l_2m_2+2c_3l_2m_3\,co\\
D(2,3) &= D(3,2)m_3c_3^2+l_2m_3\cos(q_3)c_3+I_{3z}\,,\\
D(3,3) &= m_3c_3^2+I_{3z}\,,
\end{aligned}
$$

$$
\begin{aligned}
g(1,1) &= -g(m_1+m_2+m_3)\,,\\
g(2,1) &= -C_3gm_3\cos(q_2+q_3) - g(m_2(C_2+L_2)+L_2m_3)\cos(q_2)\,,\\
g(3,1) &= -C_3gm_3\cos(q_2+q_3)\,.
\end{aligned}
\qquad (54)
$$

$$
\begin{aligned}
D(1,1) &= \Theta_1\\
D(1,2) &= \Theta_2cos(q_2)+\Theta_3cos(q_2+q_3+q_4)+\Theta_4cos(q_2+q_3)\\
D(1,3) &= \Theta_3cos(q_2+q_3+q_4)+\Theta_4cos(q_2+q_3)\\
D(1,4) &= \Theta_3cos(q_2+q_3+q_4)\\
D(2,1) &= D(1,2)\\
D(2,2) &= \Theta_5+2\Theta_6cos(q_3+q_4)+2\Theta_7cos(q_3)+2\Theta_8cos(q_4)\\
D(2,3) &= \Theta_9+\Theta_7cos(q_3)+2\Theta_8cos(q_4)+\Theta_6cos(q_3+q_4)\\
D(2,4) &= \Theta_{10}+\Theta_6cos(q_3+q_4)+\Theta_8cos(q_4)\\
D(3,1) &= D(1,3)\\
D(3,2) &= D(2,3)\\
D(3,3) &= \Theta_9+2\Theta_8cos(q_4)+m_4l_3^2+I_{3z}+I_{4z}\\
D(3,2) &= \Theta_{10}+\Theta 8cos(q_4)\\
D(4,1) &= D(1,4)\\
D(4,2) &= D(2,4)\\
D(4,3) &= D(3,4)\\
D(4,4) &= \Theta_{10}
\end{aligned}
\qquad (55)
$$

$$
\begin{aligned}
C(1,1) &= 0 \\
C(1,2) &= -\dot{q}_3(\Theta_3 sin((q_2+q_3+q_4)+\Theta_4 sin(q_2+q_3)) - \dot{q}_2(\Theta_2 sin(q_2)+\Theta_3 sin((q_2+q_3+q_4)+\Theta_4 sin(q_2+q_3)) - \Theta_3\dot{q}_4 sin(q_2+q_3+q_4) \\
C(1,3) &= \dot{q}_2(\Theta_3 sin((q_2+q_3+q_4)+\Theta_4 sin(q_2+q_3)) - \dot{q}_3(\Theta_3 sin((q_2+q_3+q_4)+\Theta_4 sin(q_2+q_3)) - \Theta_3\dot{q}_4 sin(q_2+q_3+q_4) \\
C(1,4) &= \Theta_3\dot{q}_2 sin(q_2+q_3+q_4) - \Theta_3\dot{q}_3 sin(q_2+q_3+q_4) - \Theta_3\dot{q}_4 sin(q_2+q_3+q_4) \\
C(2,1) &= 0 \\
C(2,2) &= -\dot{q}_3(\Theta_6 sin(q_3+q_4)+\Theta_7 sin(q_3)) - \dot{q}_4(\Theta_6 sin(q_3+q_4)+\Theta_8 sin(q_4)) \\
C(2,3) &= 0 \\
C(2,4) &= 0 \\
C(3,1) &= 0 \\
C(3,2) &= 0 \\
C(3,3) &= 0 \\
C(3,2) &= 0 \\
C(4,1) &= 0 \\
C(4,2) &= 0 \\
C(4,3) &= 0 \\
C(4,4) &= 0
\end{aligned}
\tag{56}
$$

TABLE III
PLANT PARAMETERS TABLE

Parameter	Value	Units
m_1	21.29	Kg
m_2	8.57	Kg
m_3	2.33	Kg
I_2	0.435	$Kg-m^2$
I_3	0.062	$Kg-m^2$
d_0	0.5	m
L_2	0.425	m
L_3	0.527	m
C_2	-0.339	m
C_3	0.320	m
g	9.81	m/s^2